Bayesian analysis of cosmic-ray propagation parameters: secondary antiparticles from spatial-dependent diffusion models

Jie Feng [1,2],* Nicola Tomassetti [3,4],† and Alberto Oliva [5]‡
[1] *Institute of Physics, Academia Sinica, Nankang, Taipei 11529, Taiwan;*
[2] *School of Physics, Sun Yat-Sen University, Guangzhou 510275, China;*
[3] *Università degli Studi di Perugia & INFN-Perugia, I-06100 Perugia, Italy;*
[4] *LPSC, Université Grenoble-Alpes, CNRS/IN2P3, F-38026 Grenoble, France, and*
[5] *Centro de Investigaciones Energéticas, Medioambientales Tecnológicas, E-28040 Madrid, Spain*

The antiparticle energy spectra of Galactic cosmic rays (CRs) have several exciting features such as the unexpected positron excess at E ∼10-200 GeV and the remarkably hard antiproton flux at $E \sim 60$–450 GeV recently measured by the AMS-02 experiment. In this paper, we report calculations of antiparticle CR spectra arising from secondary production and their corresponding uncertainties. Using the most recent data on CR protons, helium, carbon, and nuclear ratios ^{10}Be/^{9}Be and B/C, we have performed a global Bayesian analysis, based on a Markov Chain Monte Carlo sampling algorithm, under a scenario of spatial-dependent CR diffusion in the Galaxy which reproduces well the observed spectral hardening in the CR hadron fluxes. While the high-energy positron excess requires the contribution of additional unknown sources, we found that the antiproton data are consistent within the estimated uncertainties, with our predictions based on secondary production.

I. INTRODUCTION

In standard models of CR propagation, antimatter particles are only produced by by collisions of high-energy nuclei with the interstellar gas, from which the $\bar{p}/p$ ratio or the positron fraction $e^+/(e^- + e^+)$ are naively expected to *decrease* with energy as fast as the boron-to-carbon (B/C) ratio does. To interpret the positron excess, it seems to be unavoidable to introduce extra source components such as dark matter particle annihilation [1], nearby supernova remnants [2] or $e^{\pm}$ pair production mechanisms inside nearby pulsars [3]. The new AMS-02 data on the $\bar{p}/p$ ratio are also at tension with standard predictions based on secondary antiproton production. However the situation is far from being understood because conventional models of CR propagations suffers from large uncertainties and intrinsic limitations in describing the fine structures of new CR observations. For instance, recent data of CR proton and nuclei spectra revelead a high-energy departures from the standard universal power-law expectations. These features may challenge the basic assumptions of standard diffusion models and give rise to exciting questions on how, where, and why CR propagation takes place [4]. Among unjustified assumptions of traditional models, the homogenity of CR propagation has been recently questioned.

In this paper, we report the results of a complete scan of the parameter space for CR injection and propagation in order to provide a robust prediction for the $\bar{p}/p$ ratio and corresponding uncertainties. To describe the CR transport in the Galaxy, we set up a numerical implementation of a two-halo (THM) scenario of diffusive propagation [5–7], where CRs are allowed to experience a different type of diffusion when they propagate closer to the Galactic plane. To asses the uncertainties on the CR transport, we adopt a Markov Chain Monte Carlo (MCMC) sampling technique [8], using a large set of nuclear data (H, He, C, ^{10}Be/^{9}Be, B/C), which allows us to inspect parameter correlations and their degeneracies. We also review uncertainties associated to solar modulation and antiproton production cross sections. We found that the new $\bar{p}/p$ ratio measured by AMS-02 is fairly well described by a THM propagation model within the estimated errors, while the excess of e^+ require the presence of extra sources. We also give an example of one-zone diffusion models for comparison.

In Section II we give a description of the CR propagation model, the key parameters subjected to investigatoin and the method used for their determination. In Section III we report our results, we discuss the probability distribution inferred on the parameters and their degeneracy, and the overall description of CR data. We also present antiparticle spectra arising from secondary productions. The conclusions are drawn in Section IV.

II. COSMIC RAY PROPAGATION MODEL

The propagation of all CR species is described by a two-dimensional transport equation with boundary conditions at $r = r_{\rm max}$ and $z = \pm L$:

$$\frac{\partial \psi}{\partial t} = Q + \vec{\nabla} \cdot (D \vec{\nabla} \psi) - \psi \Gamma + \frac{\partial}{\partial E}(\dot{E} \psi) \,, \qquad (1)$$

where $\psi = \psi(E, r, z)$ is the particle number density as a function of energy and space coordinates, $\Gamma = \beta c n \sigma$

*Electronic address: jie.feng@cern.ch
†Electronic address: nicola.tomassetti@cern.ch
‡Electronic address: alberto.oliva@cern.ch

is the destruction rate for collisions off gas nuclei, with density n, at velocity βc and cross section σ. The source term Q is split into a primary term, $Q_{\rm pri}$, and a secondary production term $Q_{\rm sec} = \sum_{\rm j} \Gamma_j^{\rm sp} \psi_{\rm j}$, from spallation of heavier j–type nuclei with rate $\Gamma_j^{\rm sp}$. The term $\dot{E} = -\frac{dE}{dt}$ describes ionization and Coulomb losses, as well as radiative cooling of CR leptons.

In this work, we adopt a spatial dependent scenario of CR diffusion in two halos. In practice, this is made by ideally splitting the cylintrical propagation region into two z-symmetric halos characterized by different diffusion coefficients. We adopt a diffusion coefficient of the following form:

$$D_{xx}(\mathcal{R}, r, z) = \begin{cases} D_0 \beta^\eta \left(\frac{\mathcal{R}}{\mathcal{R}_0}\right)^\delta & (|z| < \xi L) \\ \chi D_0 \beta^\eta \left(\frac{\mathcal{R}}{\mathcal{R}_0}\right)^{\delta F(r,z)} & (\xi L < |z| < L) \end{cases} \quad (2)$$

where $F(r, z)$ is used to set a smooth transition between the two diffusion regions. The parameter D_0 sets the normalization of the diffusion coefficient in the disk, at the reference rigidity $\mathcal{R}_0 \equiv 0.25\,\mathrm{GV}$, while χD_0 is that in the outer halo. The low-energy diffusion is shaped by the factor β^η, where η is set to be -0.4 [9]. The parameter δ represents the scale index of the power-law dependence of the diffusion coeffient in the inner halo (with $|z| < \xi L$) while $\delta + \Delta$ is that of the outer halo ($\xi L < |z| < L$), where L is the half-height of the whole diffusion region.

In this work, we use the data to constraint the parameters of CR transport in the two regions, namely D_0, χ, δ, Δ, L and ξ. We also employ the parameter ν describing the proton injection index, and $\Delta\nu$ for the injection index difference between proton and other primary nuclei (He, C, O, ... Fe).

III. RESULTS

The best fit parameters can reproduce the primary spectra very well. Figure 1 shows the spectra of of proton, He and C, where the THM fit is plotted as dashed lines and the shaded areas represent the 1-σ (green) and 2-σ (yellow) uncertainty bands. Our results are nicely consistent with the trends obtained in former analytical derivations [5]: following the trend of the data, the spectra get progressively harder at energies above $\sim 200\,\mathrm{GeV/n}$. In the figure, the thin solid lines represents the prediction from the standard one-halo (OHM) scenario, shown for reference, which is fitted to data at energie $E \lesssim 200$ GeV/n.

The top plot of Fig. 1 shows us that THM predicts the primary particle spectra with the same quantity of deviation from a single pow-law spectra. This is expected because the primary particles propagate in the disk and halo results in $\phi_p \sim Q/D$, with $\frac{1}{D} = \frac{L}{D_0 R^\delta}(\xi + \frac{1}{\chi R^\Delta})$. The middle plot of Fig. 1, however,

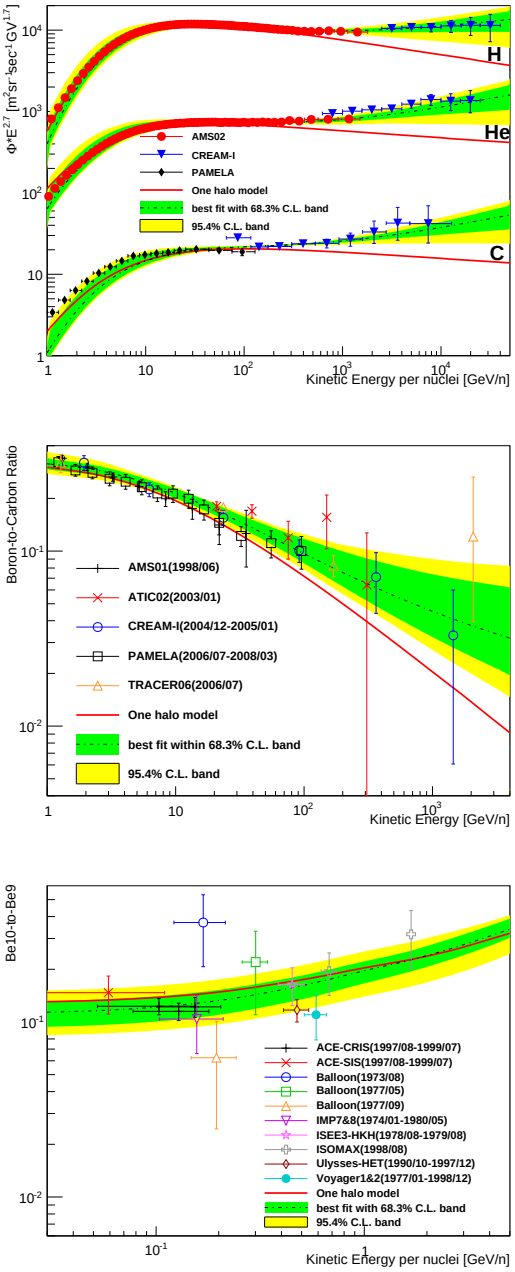

FIG. 1: Top: Model prediction of proton, He and C fluxes compared with data. Middle: Prediction of B/C compared with data. Bottom: Prediction of ^{10}Be/^{9}Be compared with data.

shows us that the secondary particle spectra has a larger high energy break than primary ones: a larger break of B than that of C results in the hardening behavior in B/C. This has also been pointed out in [6]. One should also notice that nuclear fragmentation cross section will introduce uncertainties [14, 15].

The correlation between ξ and L is also shown in the contour plot of Fig. 2. Even though we have included

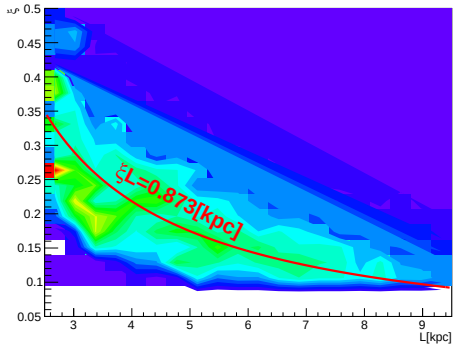

FIG. 2: Contour in the ξ and L plane. The red solide line at $\xi \times L = 0.873$ [kpc] is to guid the eye.

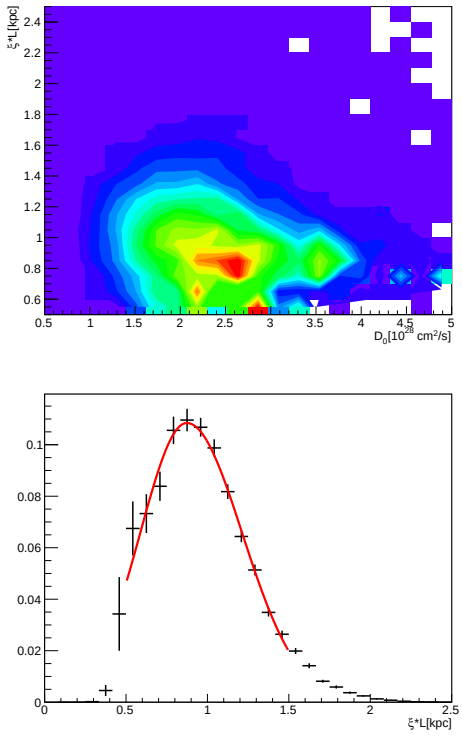

FIG. 3: Top: Contour in ξL and D_0 plane. Buttom: distribution of ξL.

^{10}Be/^{9}Be data in our study, the size of halo L does not converge.

This is illustrated in Fig. 2, showing the convergence of the inner halo height ξL to the value of ~ 1 kpc. In Fig. 3 we directly plot the contour in the (ξL - D_0) plane: it can be see that no significan correlation is present between ξL and D_0. Also, we have performed a fit on the ξL distribution in the interval $\xi L \in [0.5, 1.5]$ (kpc) with an asymmetric gaussian function, as shown in Fig. 3. The fit discribes the distribution quite well with $\chi^2/d.f. = 8.15/8$, with a mean value of $(0.873^{+0.340}_{-0.286})$ kpc.

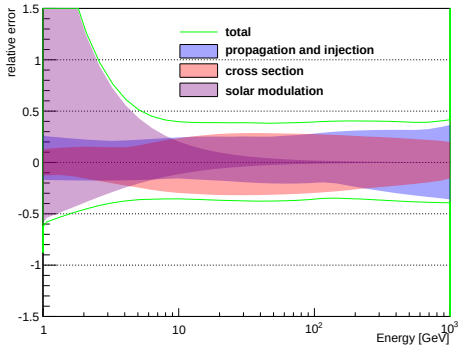

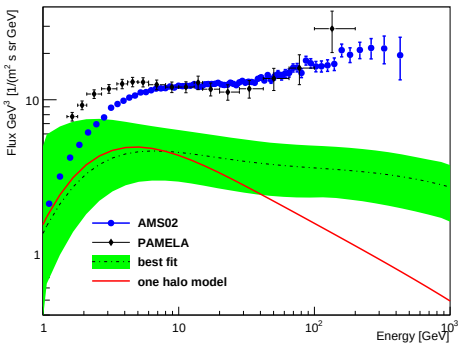

FIG. 4: Top: $e+$ flux prediction error break down. Buttom: Model prediction of positron flux compared with the experimental data by AMS-02 [10] as well as PAMELA [11].

Positron flux predicted by THM is shown in Fig. 4. The positron flux predicted by THM is harder than that by OHM. One can expect this because positron spend a larger fraction of time in the disk in THM where the δ is smaller than that in OHM. We give a break down of the errors from the model. The cross section error is estimated as in [16].

The antiprotons emitted in p-p(ISM), p-He(ISM), He-p(ISM) and He-He(ISM) collisions are characterized by broad energy distributions and large inelasticity factors. Antineutrons produced from the above collisions also decay to become antiprotons. The transport properties of antiprotons in the Galaxy is similar to that of protons. However, non-annihilating reactions of secondary $\bar{p}$ with the gas may also produce a further energy shift toward lower energies. Comparing the MC generator models with the most recent experimental data [17], we validate EPOS LHC [18] as the best one and use it in this work. Apart from the propagation and cross section errors discussed above, we also need to consider solar modulation error especially for low energies. Comparing to the antiproton flux, $\bar{p}/p$ is a better observable to eliminate most of the solar modulation and the proton normalization uncertainties. The top graph of Fig. 5 shows the

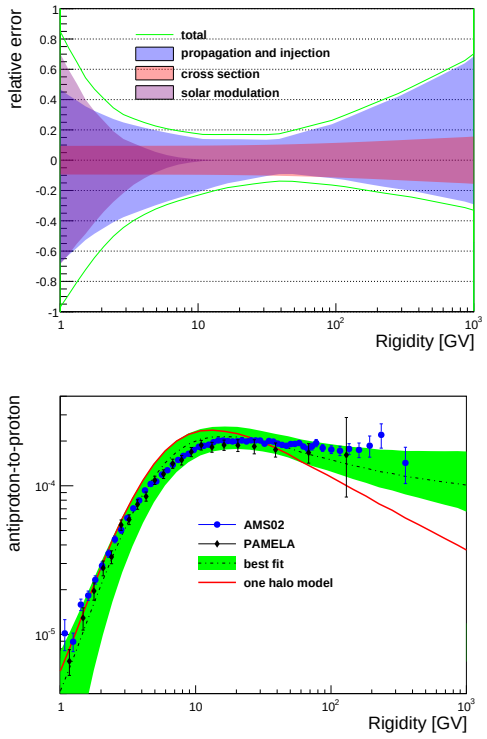

FIG. 5: Top: $\bar{p}$ prediction error break down. Buttom: The $\bar{p}/p$ ratio as function of rigidity R. The model calculations are shown in comparison with the AMS-02 [12] and PAMELA [13] data.

break down of the $\bar{p}/p$ prediction errors.

The $\bar{p}/p$ ratio is shown for the two considered models in the bottom graph of Fig. 5. In OHM, it decreases smoothly above $\sim$ 10 GeV. In our THM, the ratio has a flattening tendency at $E \sim 10$ GeV to $\sim$ 100 GeV.

IV. CONCLUSIONS

Here we summarize everything. We estimate the inner halo size, namely disk height, of our galaxy to be around 1 kpc. The outer halo size should be further studied. The Bayesian analysis gives us the uncertainty band from propagation and nuclei injection. We also study the antiproton production cross sections carefully and validate EPOS LHC model. We show the error break down of the antiparticle predictions. The uncertainties from $\bar{p}/p$ measurement by AMS-02 are already smaller than those from model predictions. It is shown that there is no room for extra source to produce antiprotons. Positron prediction shows that there is a hint of the existence of extra sources which produce or accelerate positrons but not secondary nuclei.

Acknowledgments

JF acknowledges the Taiwanese Ministry of Science and Technology (MOST) under Grant No. 104-2112-M-001-024 and Grant No. 105-2112-M-001-003. NT acknowledges the European Union for support under the H2020-MSCA-IF-2015 action, grant agreement No. 707543-MAtISSE. AO acknowledges CIEMAT, CDTI and SEIDI MINECO under Grants ESP2015-71662-C2-(1-P) and MDM-2015-0509.

[1] M. Cirelli and A. Strumia, ArXiv e-prints (2008), 0808.3867.
[2] N. Tomassetti and F. Donato, Astrophys.J. **803**, L15 (2015), 1502.06150.
[3] J. Feng and H.-H. Zhang, Eur. Phys. J. **C76**, 229 (2016), 1504.03312.
[4] P. Blasi, Astron. Astrophys. Rev. **21**, 70 (2013), 1311.7346.
[5] N. Tomassetti, Astrophys. J. **752**, L13 (2012), 1204.4492.
[6] N. Tomassetti, Phys. Rev. D **92**, 081301 (2015), 1509.05775.
[7] Y.-Q. Guo, Z. Tian, and C. Jin (2015), 1509.08227.
[8] A. Lewis and S. Bridle, Phys. Rev. D **66**, 103511 (2002), astro-ph/0205436.
[9] D. Gaggero, L. Maccione, D. Grasso, G. Di Bernardo, and C. Evoli, Phys. Rev. D **89**, 083007 (2014), 1311.5575.
[10] M. Aguilar et al. (AMS), Phys.Rev.Lett. **113**, 121102 (2014).
[11] O. Adriani et al. (PAMELA), Phys. Rev. Lett. **111**, 081102 (2013), 1308.0133.
[12] M. Aguilar et al. (AMS Collaboration), Phys. Rev. Lett. **117**, 091103 (2016), URL http://link.aps.org/doi/10.1103/PhysRevLett.117.091103.
[13] O. Adriani et al., JETP Lett. **96**, 621 (2013), [Pisma Zh. Eksp. Teor. Fiz.96,693(2012)].
[14] N. Tomassetti, Phys. Rev. C **92**, 045808 (2015), URL http://link.aps.org/doi/10.1103/PhysRevC.92.045808.
[15] N. Tomassetti, Astrophys. Space Sci. **342**, 131 (2012), 1210.7355.
[16] T. Delahaye, F. Donato, N. Fornengo, J. Lavalle, R. Lineros, P. Salati, and R. Taillet, Astron. Astrophys. **501**, 821 (2009), 0809.5268.
[17] J. Feng, N. Tomassetti, and A. Oliva, Phys. Rev. **D94**, 123007 (2016), 1610.06182.
[18] T. Pierog, I. Karpenko, J. M. Katzy, E. Yatsenko, and K. Werner, Phys. Rev. C **92**, 034906 (2015), 1306.0121.